Asian Journal of Water, Environment and Pollution, Vol. 7, No. 3, pp. 49-67.

Inorganic Elements and Radioisotopes in the Environment: Measurement Techniques and Applications

M. Someshwar Rao*, Bhishm Kumar and U.K. Singh

Hydrological Investigations Division, National Institute of Hydrology, Roorkee, India

✉ somesh@nih.ernet.in

Received May 9, 2008; revised and accepted July 23, 2009

Abstract: In this review paper, modern nuclear techniques are discussed for the analysis of inorganic elements or tracers, including radioactive species in the environment. Nuclear techniques allow many trace elements to be analyzed in parts per 106 to parts per 109 range in both field and laboratory measurements. For laboratory and in-situ field measurements, techniques of X-ray fluorescence (XRF), particle induced X-ray emission (PIXE), neutron activation analysis (NAA) and radionuclide detection using NaI(Tl) spectrometer, Ge(Li), Si(Li), silicon drift detector (SDD) spectrometer and HPGe spectrometer are discussed. The paper also includes some of the studies carried out using these techniques in various parts of the world. These studies are important not only from the environmental contamination point of view, but also for various other applications.

Key words: Radionuclide, environmental pollution, XRF, PIXE, NAA, NaI(Tl), Si(Li), Ge(Li), HPGe, SDD.

Introduction

Rapid growth in population and industrialization has resulted adversely on the environment. Many inorganic elements and radioisotopes are found in the environment. One of the main sources of irradiation to the human body is gamma radiation (terrestrial environmental background radiation) emitted by naturally occurring radioisotopes. The most prominent naturally occurring radioisotopes are ^{40}K and the radionuclides from the ^{232}Th and ^{328}U series with their decay products, which exist at trace levels in ground formations. In addition to the naturally occurring radionuclides in ground formations, a large number of radioisotopes are also produced in our atmosphere due to cosmic rays interactions (Lal D., 1998). The testing of atomic devices and accidents which occur in nuclear power plants are also the major source of increased activity of various radioisotopes in our atmosphere including effluents from the reactors that contaminate water bodies and ground formations (Gudiksen et al., 1989). However, this activity can be used for various applications and investigations. Over the last few decades, extensive surveys have been carried out worldwide to determine activity concentration levels and associated dose rates to terrestrial gamma radiation (UNSCEAR 2000 report). In US, per capita radiation dose from medicine (through interventional, radiography, nuclear medicine and CT scanning) in 2006 is 3 mSv which exceeds even the natural radiation exposure rate of 2.4 mSv (Mettler, 2008). Gamma emitting radionuclides are also the most widely used radiation sources. For example, irradiation of food for sterilization of packaged food is widely used in large parts of the world. The penetrating power of gamma photons has many applications. Some of the useful gamma ray emitting environmental radionuclide is given in Table 1. Such investigations are important not only for assessing population exposure and performing epidemiological studies, but also for serving as a reference (base line data) to possible environmental contaminations due to human activities.

*Corresponding Author

Table 1: Environmental radionuclides

Single γ-ray (Half life)	*Multiple γ-ray (Half life)*	*Coincidence γ-ray (Half life)*
^{7}Be (53.28 d)	^{57}Co (270.9 d)	^{22}Na (950.97 d)
^{40}K (1.3×10^{9} Y)	^{58}Co (70.77 d)	^{46}Sc (83.831 d)
^{51}Cr (27.7 d)	^{59}Fe (44.5074 d)	^{60}Co (1925.2 d)
^{54}Mn (312.028 d)	^{65}Zn (244.164 d)	^{88}Y (106.626 d)
^{95}Nb (35.15 d)	^{95}Zr (64.02 d)	$^{110\,m}$Ag (249.95 d)
^{103}Ru (39.31 d)	^{106}Rh (29 s)	^{124}Sb (60.2 d)
^{137}Cs (11018.3 d)	^{125}Sb (1007.56 d)	^{134}Cs (753.88 d)
^{141}Ce (32.51 d)	^{131}I (8.0197d)	^{140}La (40.293 h)
^{144}Ce (284.534 d)	^{140}Ba (12.7527 d)	^{152}Eu (4947.2 d)
	^{144}Pr (17.28 m)	^{207}Bi (11523 d)
	^{155}Eu (1739.06 d)	

Modern nuclear techniques are extensively used for the analysis of inorganic elements and radioisotopes in the environment under field and laboratory. The purpose of this paper is to popularize the nuclear techniques which can be used to detect inorganic elements and radioisotopes in the environment for environmental contamination studies, groundwater and surface studies, oceanography, soil studies, archeology, present and past climate studies etc. These nuclear techniques include field instrumentation (X-ray fluorescence, neutron activation analysis and radionuclide detection) and laboratory instrumentation (NaI(Tl), Ge(Li) and HPGe detectors).

Methods

The nuclear analytical methods which are discussed in this paper are based on the detection of X-rays or photons emitted from the subject element. These emissions may be associated with primordial, cosmogenic or artificially produced radioactive species, or may arise from the decay of radio-elements following neutron activation, and from excitation of an element with energy such as in X-ray fluorescence analysis. These procedures allow elemental detection in ppm to ppb concentrations in environmental matrices either in field or in laboratory.

X-ray Fluorescence

X-ray fluorescence (XRF) technique is used for rapid analysis of large number of elements simultaneously at trace to high concentration level (Rieck et al., 1975). It is a non-destructive technique as the sample remains unaltered after the examination performed. The procedure involves excitation of sample by illuminating with an intense monochromatic X-ray beam. The sample in turn fluoresces to produce the characteristic X-rays derived from ionization of the component atoms. Energy of the characteristic X-rays is specific to the emitting element while intensity of the X-rays at each characteristic wavelength indicates elemental concentration (US EPA, 1999b). Since only inner electrons are involved, characteristic X-ray energies are practically independent of the physical and chemical state of the emitter. A semiconductor detector (e.g., Si(Li), HPGe or Si-drift detector) converts the energy of the incident secondary (characteristic) X-ray into a voltage pulse whose amplitude is proportional to that energy. This instrument is called Energy Dispersive Spectrometer (EDS). In a modification of the EDS technique, called Wavelength Dispersive Spectroscopy (WDS), characteristic X-rays are diffracted using a crystal spectrometer and then analyzed (Figure 1). Some of the popularly used diffracting crystals are: thallium acid phthalate (TAP), thallium(I) hydrogen phthalate (TlAP), pentaerythritol (PET), lithium fluoride (LiF), layered synthetic microstructure (LEM), ammonium dihydrogen phosphate (ADP), germanium (Ge), graphite, indium antimonide (InSb), *tetrakis*-(hydroxymethyl)-methane: penta-erythritol (PE), potassium hydrogen phthalate (KAP), rubidium hydrogen phthalate (RbAP) etc. Analytical range of some of these crystals, given in Table 2, provides X-ray lines and element range that can be analyzed.

Handy and portable XRF systems for field analysis have come up with the use of Si drift detectors cooled by Peltier elements. Field portable x-ray fluorescence (XRF) spectrometers come in two forms: one that contains radionuclides ^{109}Cd, ^{241}Am or ^{57}Co and the other contains a silver anode x-ray tube that does not contain radionuclide sources. The portable system can be

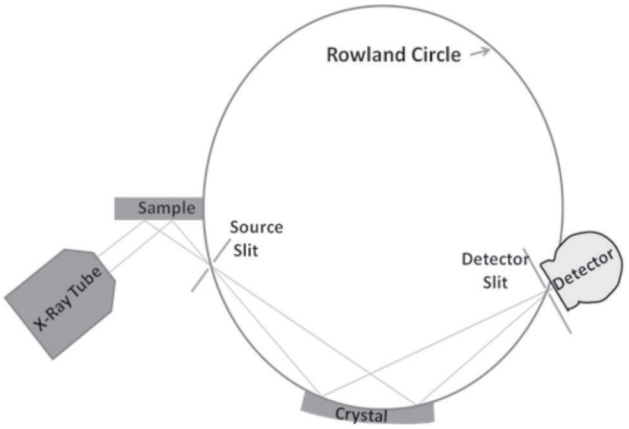

Figure 1: X-ray fluorescence analysis.

Table 2: Elemental analytical range of various diffracting crystals

Crystal name	*X-ray lines and element range*
TAP	Kα: O to P ; Lα: Cr to Nb ; Mα: Ba to Hg
PET	Kα: Si to Mn; Lα: Kr to Tb; Mα: Lu to Bi and Th-U
LIF	Kα: Ca to Y; Lα: Sb to U
ODPB	Kα: B to O; Lα: Ca to V
LDEC	Kα: B to O
PXI	Na, Mg
PE 002	Cl, S
LSM 60 (W-Si)	Kα: C to F; Lα: Ca to Fe
LSM 080 (Ni-C)	Kα: B to O
LSM 200 (Mo-B_4C)	Kα: Be to B

operated even underwater to 100 m water depths. However, laboratory analysis of high energy (50-100 KeV) X-rays are normally done using intrinsic Ge detectors due to their higher efficiency compared to Si(Li) detectors. WDS provides high spectral resolution (2-20 eV) but the peaks are occupied sequentially while EDS has less energy resolution (70-130 eV), but has the advantage that all spectral lines are accumulated simultaneously, giving a complete analysis in ~20 seconds. High spectral resolution allows WDS to detect elements an order of magnitude lower concentration than EDS. However, data collection and analysis is quick and easy with EDS. EDS is the method of choice for qualitative "identification" analyses.

With XRF system, at least 10 samples/hour in ppm range can be analyzed from 10 to 40 elements depending on the matrix. XRF is well suited for investigation of major elements (Si, Ti, Al, Fe, Mn, Mg, Ca, Na, K, P) and trace elements (in abundance >1 ppm; Ba, Ce, Co, Cr, Cu, Ga, La, Nb, Ni, Rb, Sc, Sr, Rh, U, V, Y, Zr, Zn) in rock and sediments. EDS spectra is also used to get 2D and 3D tomographic image of minute objects with high spatial resolution (Wegrzynek et al., 2005). WDS system does not require correction for atomic number or fluorescence but requires correction for absorption. Modern X-ray systems simultaneously collect X-ray fluorescence, absorption and transmitted X-ray beam. XRF has limited ability to detect elements with $Z<11$. XRF analysis cannot distinguish variations among isotopes of an element, so these analyses are routinely done with other instruments like TIMS, SIMS, IRMS etc. Similarly, XRF analysis cannot distinguish ions of the same element in different valence states, so these analyses are done with techniques such as wet chemical analysis or Mossbauer Spectroscopy.

If the XRF analysis is carried out with X-rays incident on the sample at or below critical angle (or total reflection angle), it is termed as grazing incidence or total reflection XRF (GXRF or TXRF). GXRF or TXRF scanning allows measurement of density, roughness, layer thickness, depth profiling and also as a tool for determining ultra trace multi-elements.

The continuum background due to scattered radiation in XRF spectra can be reduced to a large extent by using high intense X-rays generated using synchrotron source (SR-XRF) coupled to an optic system to generate coherent, monochromatic, linearly polarized beam. Such beams provide high resolution images and extend the range of elements that can be analyzed (Adams et al., 1998). It has very low detection limits (down 10^{-17} g of element from boron to uranium) with spatial resolution down to 40 nm.

Particle Induced X-ray Emission spectroscopy (PIXE) is another technique similar to XRF. In this technique,

Table 3: Detection limits in EDS, WDS and PIXE measurements of glass matrix with a low Pb-content, expressed as ppm by weight

Element	*EDS*	*WDS*	*Element*	*WDS*	*PIXE*
Na	800	160	Ti	20	15
Mg	660	20	Mn	35	7
Al	330	20	Fe	30	5
Si	800	15	Cu	50	3
P	790	120	Zn	60	3
Cl	1000	30	Zr	100	3
K	1000	15	Ba	60	160
Ca	930	15	Co, Ni	—	4
			Pb, Rb, Sr	—	2

X-ray fluorescence in target atom is achieved by using energetic ion beam (e.g., proton beam in the range of 2-5 MeV) produced by an accelerator. Using energy dispersive detector elements the technique can determine simultaneously elements from sodium to uranium. Low background radiation (Bremsstrahlung) and high X-ray production cross-section are the main advantage of the PIXE method over electron excitation or X-ray fluorescence (XRF). The measuring time using the PIXE method is about 3 min for each sample and each element.

Similar to the technique PIXE is the Proton Induced Gamma Ray Emission (PIGE). The lower Coulomb barrier of light elements makes PIGE suitable for the analysis of light elements such as ^{7}Li, ^{9}Be,^{11}B, ^{19}F, ^{28}Si, ^{35}Cl, ^{23}Na and ^{27}Al.

Electron probe micro analysis (EPMA) or simply electron microprobe is similar to XRF. In this technique, X-rays are generated from the material to be analyzed by electron impact. In quantitative electron microprobe analysis, corrections are needed for atomic number effects (Z), absorption (A) and fluorescence (F). Further details on scanning electron microscopy and X-ray micro-analysis can be seen in Goldstein et al. (2007).

Neutron Activation Analysis (NAA)

Neutron activation technique is a multi-elemental analytical technique used for both qualitative and quantitative analysis of more than 70 elements at trace concentrations in solids, liquids, suspensions, slurries and gases with no or minimal sample preparation. Neutron activation analysis involves bombardment of a sample and a standard with a high neutron thermal flux (thermal neutron $E \sim 0.025$eV), epithermal neutrons (E = 0.5 to 100 keV), fast neutrons (E = 100 keV to 25 MeV) in a nuclear reactor or accelerator. The elements in the sample are transformed into radioactive isotopes that emit gamma and beta radiation. The gamma rays are more frequently monitored since they are discrete and characteristic of the emitting isotopes. The measured intensities of the gamma rays are proportional to the amounts of elements present. NAA is a simultaneous, multi-element method and does not require significant sample preparation such as extraction or digestion. NAA can detect ppb levels of impurities of Dy, Eu, In, Lu, Mn, Au, Ho, Ir, Re, Sm, W, Ag, Ar, As, Br, Cl, Co, Cs, Cu, Er, Ga, Hf, I, La, Sb, Sc, Se, Ta, Tb, Th, Tm, U, V and Yb. The measurement accuracies are usually within 5% with the precision better than 1%. The major disadvantages of the technique are the availability of suitable neutron activation sources or nuclear reactors and the disposal of the sample that becomes radioactive on irradiation.

In-field analysis of terrestrial, saline and freshwater elemental analysis have become possible with the advent of artificial isotope ^{252}Cf, which decays by spontaneous fission with associated neutron emission. The system involves a ship-board system containing ^{252}Cf source and its associated Ge(Li) detector. The system is useful in rapid in-situ analysis of selected trace elements.

Detectors for Radiation (X-Ray and γ-Ray) Detection

A good detector produces spectral data that contains all the peaks of interest with each peak well defined with high signal to noise ratio and no spectral interference from neighbouring species. Of the several possible radiation detectors, we are discussing here mainly scintillation detector NaI(Tl) and semiconductor detectors (intrinsic Ge, Ge(Li) and Si(Li)). These are amongst the most popular and widely used in different fields of sciences. With these detectors it is possible to detect radioactive pollutants, natural fall out species or tracers in water and their associated sediments at few hundred dpm level concentration (Neilson et al., 1976). In general, closer the sample to the active area of detector higher is the counting efficiency.

NaI(Tl) Detector

The energy resolutions of standard 3" × 3" NaI(Tl) detectors are frequently in the 7.5% to 8.5% range for 662 keV photons from ^{137}Cs decay. The thickness of the NaI(Tl) crystal is selected on the basis of photon spectrum to be detected. Thicker crystal can absorb higher energetic photons and therefore provide higher energy resolution. However, due to increased crystal imperfection with crystal size, the background increases with crystal dimension and this lowers the limit of detection. Another important factor that contributes to the detection efficiency is the signal loss between the NaI(Tl) crystal and the photomultiplier tube. This is normally controlled by applying silicone grease that has refractive index about 1.465. By using coincidence and anti-coincidence counting technique radioactive element emitting a single photon; multiple photons in coincidence and species that emit multiple photons which are in a time coincidence (see Table 4) can be separated. Prior to sample analysis, the system is calibrated using standard gamma ray sources such as ^{60}C, ^{241}Am, ^{137}Cs, ^{90}Sr, ^{133}Ba, ^{208}Tl etc. for its channel number versus gamma ray energy. The calibration curve is then used to convert the gamma emissions observed at different channel number into the energy spectrum. Modern high-resolution gamma-ray

Table 4: Some important properties of NaI(Tl)

Density:	3.67 g/cm^3
Hardness:	2 Mohs
Hydroscopicity:	Very hygroscopic
Radiation length:	2.6 cm
Pulse Amplitude is linear over	0.1 to 2 MeV
Flatness:	λ/4 @ 633 nm
Light escape cone to air:	44.7°
Time resolution (for ^{60}Co):	1000 ps
Optical transmission range:	250 nm to 35 μm
Decay constant:	Fast 620 ns Slow 250 ns
Energy resolution (for 662 keV of Cs):	about 6.7%
Linear attenuation coefficient for γ-rays: at 511 keV: 0.34 cm^{-1}; at 100 keV: 5.5 cm^{-1}	
Refractive Index (Maximum emission wavelength): 1.85	
Emission wavelength: Fast 310 nm Slow 410 nm	
Light yield: Fast 6.5×10^3 Slow 4×10^4 photon/MeV	

cameras have come up with the combined pixallated NaI(Tl) crystal and position sensitive photomultiplier tube (PSPMT) (Qi et al., 2002).

Si(Li) Detector

Si(Li) semiconductor detectors consist of a 2 to 5 mm thick Si crystal with gold contacts at its ends, a "Li-drifted" intrinsic region facing the specimen and an adjacent Li-free region. The front contact, Li-drifted intrinsic region, and Li-free region constitute a p-i-n junction. A bias is applied across the crystal and a current flows (Figure 2). The crystal is maintained at low temperatures to prevent diffusion of Li from the intrinsic region to the Li-free region.

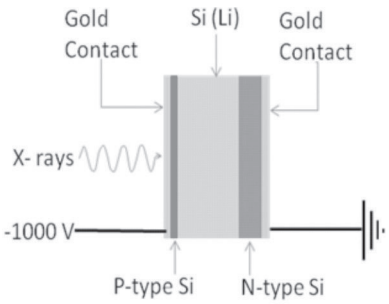

Figure 2: Si(Li) detector.

On interaction of X-ray with the crystal, free charges are produced that conduct current due to the bias placed across the crystal. The total charge conducted is directly proportional to the energy of the absorbed X-ray. To reduce the leakage current, noise and background the detector is sheathed in a liquid-N_2-filled cryostat. Li is an electron donor and its presence makes the Si crystal a better semiconductor and swamps out the effects of impurities. Li-drifted crystals are called "silly" for Si(Li) and "jelly" for Ge(Li).

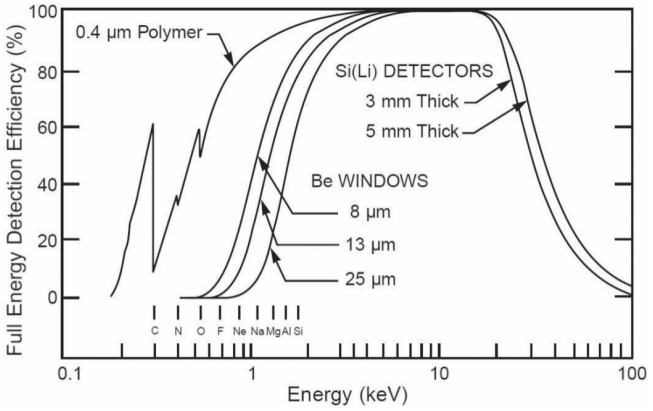

Figure 3: Transmission curves for various types and thickness of windows. The polymer window curve does not show the effect of the support grid on overall efficiency.

Ge(Li) Detector

Ge (Li) detector is a closed-end coaxial crystal with an active volume ~ 60 cm^3, mounted in an aluminium cap. It is connected to a resistive feed-back preamplifier. The block diagram of the electronics is shown in Figure 4. The resolution of Ge(Li) detector is ~2.3 keV at 1.33 MeV. The efficiency of the system marginally deteriorates with time (~2% in three years for ^{60}Co signal). Ge(Li) detector has a better resolution than that of NaI(Tl) crystal system; however, its efficiency is lower.

A comparison between NaI(Tl) and Ge(Li) for minimum detection level for various isotopes (Table 5) shows these two systems are mostly identical for each radioisotope except in few cases. Both Ge(Li) and NaI(Tl) systems can simultaneously identify 20 to 25 radio-nuclides from fall-out with their coincidence or routing techniques.

HPGe Detector

High purity germanium (HPGe) detectors have high efficiency and high energy resolution than NaI(Tl) and Ge(Li) spectrometers. In HPGe detectors, impurity level is very low i.e., 10^{10} atoms/cm^3. Techniques have been developed to achieve this goal in germanium, but not in silicon. At this impurity level in germanium, a depletion depth of 10 mm can be reached using a reverse bias voltage of less than 1000 V. The HPGe detectors are enclosed in an evacuated metal can and maintained at –196°C using a cold finger immersed in liquid nitrogen.

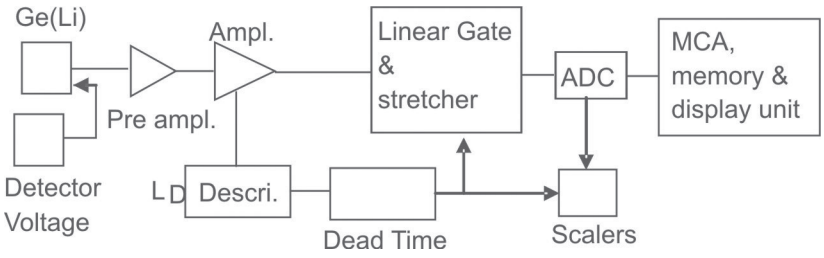

Figure 4: Block diagram of Ge(Li) detector.

Table 5: Minimum detection level (pCi/l) for reactor effluent radionuclides using NaI(Tl) and Ge(Li) detectors for 30 min counting time

Isotope	*Energy (KeV)*	*Half life*	*(pCi/l)*	
			NaI(Tl) (7.5×7.5 cm)	*Ge(Li) (65 cc)*
^{24}Na	1369	14.9512±0.0032 h	6.6	7.0
^{51}Cr	320	27.701±0.0012 d	64.0	42.0
^{54}Mn	834	312.028±0.034 d	5.2	5.4
^{56}Mn	847	2.58 h	5.4	5.6
^{59}Fe	1095	44.5074±0.0072 d	6.6	9.6
^{58}Co	810	70.77±0.11 d	5.6	5.2
^{60}Co	1332	1925.20±0.25 d	5.6	7.0
^{64}Cu	511	12.7 h	13.0	12.0
^{65}Zn	1115	244.164±0.099 d	11.0	14.0
^{103}Ru	497	39.310±0.044 d	5.5	4.8
^{106}Rh	512	1.02 y	23.0	21.0
^{137}Cs	622	11018.3±9.5 d	4.7	37.0
^{140}Ba	537	12.7527±0.0023 d	14.0	13.0
^{140}La	1596	40.293±0.012 h	14.0	13.0

Incident gamma rays from the material to be analyzed produce electron hole pairs which are collected by an applied electric field of strength 1-5 kV DC. The output pulse is proportional to the amount of energy deposited. With fast pulse shaping, AC power line compensator and signal processing circuit, stable and well resolved peaks even at count rates as high as 10^5 cps can be measured. The entire detector is shielded from external radiation using "old lead" with inner lining of thick copper to reduce lead X-rays and backscatter photons originating from the shield walls. HPGe detectors are available in various configurations (Figure 5). The active area of the detector comes in various forms such as in concentric cylindrical shape popularly known as coaxial configuration. The detector can contain beryllium or carbon fibre cryostat window to allow passage of low energy gamma rays (carbon fibre has 70% transmission at 10 keV. Beryllium has 23% higher transmission at 10 keV, but it is fragile). FWHM of extended range coaxial Ge detector at 22 keV range is 0.7 to 1.2 keV. Energy range of some of the detector is given in Table 6. High resolution and high sensitive HPGe detector with 4π-imaging capability are used widely in biomedical research (Todd et al., 1974; Niedermayar et al., 2005), astrophysics (Schoenfelder et al., 1973), national security such as nuclear non-proliferation (Neidermayer et al., 2005), hydrology etc.

Silicon Drift Detector (SDD)

It is high purity silicon with a very low leakage current and low electronic noise. The detector works high purity allows it to use at room temperature and at –10°C (using Peltier cooling) it provides excellent spectroscopic results (leakage current at 300K is ~1 nA/cm^2). The energy resolution for 7 mm^2 × 450 µm active area is 136 eV at 5.9 keV (^{55}Fe) for 9.6 µS peaking time counting. Peak to Background ratio (P/B) at this peaking time is 7000/1.

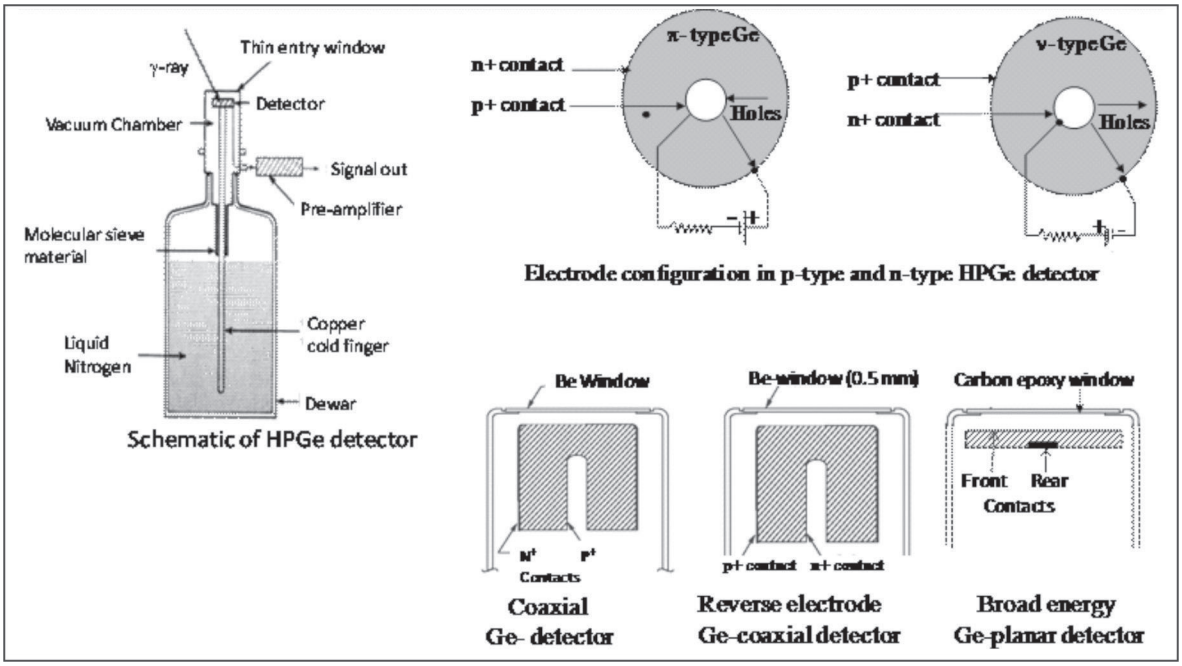

Figure 5: Various detector configurations.

Table 6: Energy range of operation and resolution of Si(Li) and HPGe detectors

Detector type	*Dead layer*	*Energy range of operation*	*Resolutions*		
			At 5.9 keV	*At 122 keV*	*At 1.33 MeV*
Li-drifted Si-planar	180 Å	109 eV to 60 keV	150 eV	—	—
p-type HPGe planar	180 Å	180 eV to 1 MeV	300 eV	600 eV	—
n-type HPGe planar	0.3 µm	3 keV to 1 MeV	330 eV	570 eV	—
p-type HPGe coaxial	0.5 mm	40 keV to 10 MeV	—	1 keV	2 keV
n-type HPGe coaxial	0.3 µm	4 keV to 10 MeV	900	—	2 keV

With Peltier cooling, the energy resolution in terms of full-width-at half-maximum (FWHM) can be obtained up to 54 eV at F-Kα (676 eV), 123 eV at Min-Kα (5.89 keV), 143 eV for ^{55}Fe-Kα (5.9 keV), 46 eV at Cu-Kα (8.4 keV) and 185 eV at pb Lα line (10.55 keV). The Cu-Kα FWHM-line width is 223 eV at 10°C and 294 eV at 24°C. The energy range of operation is up to 30 keV. Large area SDD's (33 mm^2) are popular in multichannel XRF applications (Strüder et al., 1998).

Methods of Sampling for Environmental Radionuclides

The techniques for sample collection of radioactive materials vary and depend on the concentration of the particular radionuclide and sensitivity of the instrument available for its measurement. Many investigators (Felson and Sreekuman, 1970; Lal et al., 1969; Moore et al., 1973; Silker et al., 1971; Silker, 1975) have discussed the methods of sampling for ^{7}Be, ^{32}Si, ^{137}Cs, ^{226}Ra and the gamma emitting fission products in seawater.

Sample for XRF analysis is normally prepared as flat disc, typically of 20-25 mm diameter with thickness of few mm for higher-Z material and 30-40 mm thick for light element matrix. X-ray fluorescence data is simple to analyze. To go further down to ppb levels, samples are pre-concentrated by evaporation or freeze drying or using ion-exchange resin-loaded filter papers. Liquid sample is preconcetrated by force through nebulizer and pressurized air into a dry clean airstream where the droplets evaporate. The solid residual aerosol is collected by an impactor on a thin polystyrene film. In case of PIXE, solution is concentrated on a target film that is not affected by proton beam. The dried sample is analyzed

under X-ray (XRF) or proton beam (PIXE) and the resultant X-ray spectrum is analyzed to interpret elemental concentration. With pre-concentration using PIXE, trace element concentration down to level of ppb can be carried out using 200-500 ml sampling volumes. Analysis is based on calibration curves developed using reference samples for elements to be analyzed. For elemental detection, unknown peaks of the spectra are fitted with reference peaks acquired from reference materials. A calibration curve for peak height and elemental concentration is prepared. From the calibration curve, elemental composition and its abundance of material under study is determined. Reliable results in XRF require calibration with set of standards that have composition similar to unknown samples to avoid large extrapolations.

Applications

A few such case studies discussed below enumerate those pertaining to applications of radioisotopes and radiometric techniques in earth's and extra-terrestrial environment.

(i) Sediment Transport in Rivers

Artificial and natural radioactive tracers allow in situ continuous detection of exposed and buried particles by tracking the radiation emitted by the tracers and hence providing the information on sedimentation in water bodies, soil erosion and particle dynamics. The measurement of suspended sediment concentration (SSC) is based on the absorption or diffusion of radiations by an artificial radioactive source, or by measurement of natural gamma radioactivity emitted by the suspended sediment. Gamma ray transmission gauge that uses radioactive source (e.g. ^{109}Cd, ^{241}Am, ^{137}Cs and ^{60}Co) is highly suitable for measurement of SSC in flood events characterized by great variations in sediment concentration. Measurements based on natural radioactivity of sediments contain a gamma-ray detector (no radioactive source). The system estimates SSC on the basis of a calibration curve between suspended sediment concentration and the gamma activity contribution through it.

Using ^{137}Cs gauge detector suspended sediment load in the Calabrian basin was found to be about 1000 t/km^2 with peak rates of sediment load transport up to 1600 t/km^2. With gamma-ray retrodiffusion gauge that contains ^{137}Cs or ^{241}Am gamma source and a NaI(Tl) detector separated by a lead block, vertical profiles of sediment concentration in river stream (Tazioli, 1981) can be estimated. In the case of bed load transport, artificial radioactive tracer (e.g. ^{198}Au, ^{51}Cr, ^{192}Ir, ^{46}Sc and ^{182} Ta) is emplaced in the river with characteristics similar to those of natural sediments, and then following its movement by means of portable gamma ray detector bed load transport rate is determined. The tracer measurement provides un-interrupted signal without any disturbance to the fluid, thus giving more reliable data than can normally be obtained by other sampling techniques. Radioisotopes provide a choice of tracers with a half-life ($t_{1/2}$) over the range from few hours to few years (e.g. ^{140}La ($t_{1/2}$ = 40.2 hours), ^{51}Cr ($t_{1/2}$ = 83.9 days) and ^{130}Ag ($t_{1/2}$ = 253 days)).

(ii) Leakage from Lakes and Reservoirs

Gamma ray emitting radionuclides are useful in the identification of leakage from lakes and reservoirs. The principal advantage of gamma ray tracers is the ease with which these can be monitored in situ. The leakage from the Pszeczica reservoir (Poland) was detected by spiking eight areas of approximately 2500 m^2 by radioactive tracers ^{82}Br, ^{51}Cr and ^{131}I. The tracers were released near the bottom of the reservoir in solution of a specific gravity 1.2 g/cm^3 and at a concentration of 15×10^7 Bq/m^2 (4 mCi/m^2) (Makowski, 1967, 1970; Drost and Moser, 1983). A technique involving successive injection of tracer was used to determine the area of leakage from the Kruth-Wildenstein Barrage. Iodine-131 was employed as a tracer, using either point or continuous injection and involving activities of 7×10^9 to 8×10^9 Bq (200-500 mCi). Similar investigation at Las Lajas lake was reported by Andreu Ibrra et al. (1978). The use of emulsifying bitumen labeled by gamma ray nuclides as a tracer was used in a leakage study of the Rhine-Marne Canal, France (Molinari et al., 1970).

(iii) Sedimentation and Soil Erosion

Fallout radionuclide (e.g., ^{137}Cs, ^{210}Pb, ^{7}Be etc.) on reaching the earth's surface by either wet or dry fall out, are absorbed on the soil and become useful for tracing the movement of fine sediment. Application include the study of suspended sediment sources, sedimentation rates and sediment yield, gully erosion, floodplain sedimentation, sediment budget, residence time of sediment, redistribution of soil, and lake and reservoir sedimentation (Walling et al., 1993, 1999). Cesium-137 is an artificial radionuclide produced as a result of global fallout from the testing of nuclear weapons. With a half-life of 30.1 years, ^{137}Cs provides an average value of soil erosion for a period of about 45 years. It has been found that eroded soils lose ^{137}Cs in proportion to the

severity of erosion. At erosion sites ^{137}Cs will be present in quantities smaller than the reference value, whereas at deposition sites the opposite is observed (Yibo et al., 2008). Both ^{210}Pb and ^{7}Be are natural radionuclides that reach earth's surface via atmospheric fallout at a constant rate through time. Because of relatively short half-life, the ^{7}Be technique is useful for short-term measurements that can be related to specific events (Do et al., 2008).

The radionuclides ^{137}Cs and ^{210}Pb were determined in sediment cores originating from the flood plain of the river Yamuna, India (Saxena et al., 2002). Samples were collected at five locations: Saharanpur, Delhi, Jamanpur, Hamirpur and Allahabad, where Yamuna meets the Ganges. The rate of sedimentation derived from both the techniques, ^{137}Cs and ^{210}Pb, appeared to be quite similar. At the location Saharanpur, highest rate of sedimentation (5.99 cm/y) was found, most probably due to deforestation and other human influences in the Himalayan regions, while the lowest rate was observed in Hamirpur (2.48 cm/y). All the five cores studied showed a ^{137}Cs peak of 1963, due to radioactive fallout, caused by weapon tests. The three upstream locations (Saharanpur, Delhi and Jamanpur) showed a ^{137}Cs peak due to the Chernobyl accident. These measurement reflect that Chernobyl debris have been transferred to the low latitude river system across the Himalaya.

Global fallout ^{137}Cs was used for dating sediment cores and estimating the recent sedimentation rates (up to 1 cm/y) in the Thane Creek, which lies in the southern part of Deccan belt of India (Jha et al., 2003). The residence time of ^{210}Pb in the Thane Creek water was calculated to be 0.7 y. Further, the concentration of Pb (up to 70 μg/g) and Hg (up to 10 μg/g) in sediment profiles were measured to assess the anthropogenic input of contaminants due to industrialization, which has taken place in this area over the last two decades. The depth-wise concentration profile of Hg showed positive evidence of continued fresh input into the creek.

Rai et al. (2007) have determined the ^{210}Pb and ^{137}Cs radionuclides in sediments of Mansar lake, a natural lake located in the foot hills of Jammu and Kashmir, India. Investigators have used this study to find out the sedimentation rate in the lake. The results show that the sedimentation rate in the lake varies between 1.4 and 3.7 mm per year. With mean rate of 2.3±0.02 mm per year the sediment accumulation rate of Mansar lake is compared with that of four lesser Himalayan lakes and it is found that the Mansar lake is receiving sediment at the rate of 892.8 $m^3/km^2/yr$, which is higher than for all the lesser Himalayan lakes.

(iv) Hydraulic Characterization of Soils

Hydraulic characterization of soil is fundamental in practical agriculture. Bacchi et al. (1998) measured soil moisture and soil bulk density inside closed pressure chamber through two gamma ray beams for simultaneous determination of soil water content and soil bulk density. The procedure drastically reduces time of determination of retention curve. Barataud et al. (1999) determined water content variations in soil samples during infiltration in clay-loam forest soil using dual-energy gamma-ray apparatus. The soil water diffusivity of soil was calculated with a classical Boltzmann method. An optimization technique was used to determine the parameters of the hydraulic diffusivity model. Demir et al. (2008) used gamma-ray transmission methods to determine porosity and field capacity of soil. The radioactive sources used in the experiment were ^{241}Am, ^{133}Ba and ^{137}Cs. The mass attenuation coefficients of dry soil samples were calculated from the transmission measurements. The soil samples were irrigated by adding known quantities of water and the soil-water properties were examined.

(v) Well Logging and Aquifer Characteristic

Gamma spectroscopy system used in well logging contains 14 MeV neutron source producing 3×10^8 neutrons/s, a gamma detector and a 2048 channels MCA. From the gamma scanning of the well log, elemental composition of the strata can be determined. In general, Cl, H, Si, Ca, Fe, S, C, O, Si, Ca, Fe and S can be determined in eight minutes of counting time per measurement. Gamma spectral logs can easily discriminate radioactive species: U, Th, K and Cl. Within a stratum it is observed that as porosity increases, and as the formation water saturation ratio decreases, relative gamma-ray fluence rates increase linearly for all energies (Guiles and Dooley, 1998). Spectral gamma logging is used in hydrology to identify radioactive lithologs that mask potentially productive aquifers and in some cases provide an entry point for radon and radium into water systems. Gamma well logging is also used in radioactive tracer surveys and to measure the linear flow velocity, radial position, direction, and the flow rate of water flowing within and behind a well borehole casing. The method can also be used to quantitatively measure water flowing within a borehole in the presence of other fluids such as oil and gas (Arnold, 1995).

(vi) Water Equivalent of Snow Cover

Frozen precipitation has important implications for water quality and soil biology. Information on the snow cover is an important hydroclimatic parameter. Data on the

water equivalent of the snow cover are essential in assessing regional and global water balances. Nuclear techniques are used for accurate and rapid measurement of water equivalent of snow cover (Danilin and Dubinchuk, 1983). Techniques and devices for measurement of snow cover are (i) the absorption of gamma radiation from isotope sources (the gamma ray or gamma penetration method), (ii) the scattering of neutron radiation from isotope sources (the neutron-neutron method), (iii) the absorption of natural gamma radiation from the soil and the ground (the airborne gamma survey method) and (iv) the absorption of cosmic radiation (Friedman, 1968). A comparative study of traditional and "cosmic" measurements at the snow avalanche station of Charam-Kul, situated in the Tadzhik, of the then Soviet Socialist Republic at a height of 2800 m above sea level was carried out. The total relative error of the measurement at $d > 350$ mm was obtained within 10% (Avdyushin et al., 1979; Kogan et al. 1976), and the method was suggested to be suitable for water equivalents in the range 300-10,000 mm. Fridman (1979) has proposed a modification of this method, whereby only the neutron component of the cosmic radiation is recorded. Bland et al. (1997) used mixed Eu-152, 154 gamma ray source to assess snow water equivalent. Automated systems involve combination of airborne gamma methods and automatic snow gauge ground devices using the gamma or cosmic radiation absorption technique.

(vii) Radioactivity in Coastal Waters

Lal et al. (1976) have determined ^{32}Si specific activities in coastal waters of the world oceans. ^{32}Si is a cosmogenic radionuclides with half life of 132±13 yrs (Chen et al., 1993). This isotope was first detected in a silicious sponge collected from the coast of California (Lal et al., 1960). The ^{32}Si specific activities are found very high (35-76 dpm/kg) in the coastal sponges from the Atlantic waters, especially in the Arctic region, and those from the northwest Pacific Ocean at middle latitude. The Antarctic water sponges have very low specific activities (4-7 dpm/kg); mid-Pacific and Indian Ocean waters have intermediate values, 10-30 dpm/kg. ^{32}Si is used in understanding mixing of waters in the coastal regions and in estimation of age of groundwater. ^{32}Si provides precise dating of ice-cores and sediments (Fifield and Morgenstern, 2009).

From the measurement of gamma ray emitting radionuclides in off the Sindh Coast, Arabian Sea, Akram et al. (2006) provided baseline information on radionuclide concentration in shallow sea sediments. This data is useful for tracking pollution inventories from unusual radiological events (if any) in the territorial water of the studied region. The activity concentration measured (in Bq/kg) in various sediment samples off the Sindh Coast has been found to vary from 15.9 to 30.5 for ^{226}Ra, from 11.7 to 30.9 for ^{228}Ra and from 295.2 to 748.4 for ^{40}K. The calculated mean values of radium equivalent activity, absorbed dose rate and effective dose rate were 98 Bq/kg, 49 nGy/h and 0.06 mSv/y, respectively. No artificial radionuclides were detected in the samples measured from the study area.

(viii) Submarine Groundwater Discharge (SGD) and Coastal Currents

Submarine groundwater discharge into the coastal zone represents an important pathway for material transport. It is also an important process for management of freshwater resources in coastal region. Burnett and Dulaiova (2003) carried out the assessment of material fluxes by monitoring radon in coastal zone waters over time periods from hours to days. Changes in the radon inventories over time were converted to fluxes after making allowances for tidal effects, losses to the atmosphere, and mixing with offshore waters. The calculated radon fluxes were converted to water fluxes by dividing by the estimated or measured ^{222}Rn pore water activity. The short-lived radium isotopes (^{223}Ra and ^{224}Ra) were used to assess mixing between near-shore and offshore waters. The experiment was carried out in the coastal Gulf of Mexico. It was shown that the mixing loss derived from the ^{223}Ra gradient agreed very favourably to the estimated range based on the calculated radon fluxes. Groundwater discharge was also estimated independently by the radium isotopic approach and was within a factor of two of that determined by the continuous radon measurements and an automated seepage meter deployed at the same site.

^{222}Rn is an ideal tracer for studying SGD since its concentration in groundwater is several orders of magnitude higher than in seawater. Povinec et al. (2008) in their study monitored ^{222}Rn and four natural radium isotopes (^{223}Ra, $t_{1/2}$ = 11.4 d; ^{224}Ra, $t_{1/2}$ = 3.66 d; ^{226}Ra, $t_{1/2}$ = 1600 y and ^{228}Ra, $t_{1/2}$ = 5.75 y) as a tracer for the assessment of groundwater discharge, coastal water exchange rates in coastal zones, and for estimation of residence time of water at Flamengo and Picinguaba Bays of Brazil. The average near-shore SGD rate estimated from the continuous measurements of ^{222}Rn decay products was 17±10 cm/d. Integrated coastal SGD flux estimated for the Ubatuba coast using radium isotopes was about 7×10^3 m^3 d^{-1} per km of the coast. The radium isotope data showed scattered distributions with offshore

distance, which implied that seawater in a complex coast with many small bays and islands was influenced by local currents and groundwater/seawater mixing. The ^{222}Rn concentration analysis at offshore of Donnalucata, SE Sicily and Ubatuba, SE Brazil indicated an inverse correlation between the ^{222}Rn concentration versus tides. From high (5.6 m) to low (4.4 m) tide the ^{222}Rn in seawater varied from 1 kBq m^{-3} to 5 kBq m^{-3}. The observation was explained as the change in ^{222}Rn concentration associated with sea level changes. During the sea level change, the tides induce variations of hydraulic gradient, which increases ^{222}Rn concentrations during a falling tide, while during a high tide, ^{222}Rn concentrations decrease.

(ix) Sediment and Contaminant Transport Associated with Coastal Currents

Deep-ocean accumulation of sediment associated nuclides from the coastal discharge of radioactivity was examined by Osterberg et al. (1965) using chromium-51 as a radioactive tracer. The study was carried out in Columbia River water near its discharge into the sea. The plume of the Columbia River was traced up to 350 kilometres into sea by measuring its chromium-51 content. This radioactive tag, introduced into the river by nuclear reactors at Hanford, Washington, is used for determining rates of transport and mixing, and for identifying plume waters in the presence of other sources of fresh water.

Knoth et al. (1976) analyzed elements of economic interest near shore sands using XRF. The sensitivity for detection was less than few percent to ppm levels. The analyzed elements were As, Br, Cr, Co, Cu, Fe, Hg, Mn, Mo, Nb, Ni, Pb, Rb, Se, Sr, Y, Zn, Zr, etc.

For the purpose to identify potential processes responsible for trace element cycling (sources, redistribution and exchange) in saltwater marshes and with their coastal waters, natural radionuclides in the uranium and thorium series were measured in solid tidal phases (suspended particles, bottom sediment, surface microlayer colloids) of a salt marsh in lower Delaware (Church et al., 1986). Concentrations of U, Th, ^{210}Pb and ^{210}Po on the tidal solid phases were used to understand the mechanism by which tidal marshes appear to be trapping the nuclides into their interiors.

Sediments contaminated by discharges from nuclear facilities situated upstream of rivers may eventually reach the estuary zones. In order to understand the radionuclide diffusion, a 'naturally' contaminated river sediment (1000 kBq.kg^{-1} dry weight of ^{137}Cs) was examined for 'passive diffusion' from sediment cores to fresh water and sea water under similar physical conditions (Christensen et al., 1998). The results showed that the distribution coefficient decreases with at least a factor of 4-7 if the fresh water sediment comes into contact with high salinity sea water.

Radionuclides (^{99}Tc, ^{125}Sb, ^{90}Sr and ^{137}Cs) discharged from La Hague and Sellafield nuclear fuel reprocessing plant in France have been used to trace advection and dispersion of water masses and contaminants in the "European Coastal Current" from the English Channel to the Baltic (Dahlgaard, 1995: Harman et al., 1995). Time-series of radionuclide measurements in water samples taken in the English Channel, at the Netherlands coast, in the German North Sea sector and in Danish waters were compared with reported discharge values. It was concluded that 10% of the La Hague discharge is transported through Kattegat and that 1/3 of the inflowing Kattegat bottom water originates from the coastal current. Spatial and temporal distributions of radionuclide ratios were also used to calculate transit times from the English Channel to the coast of Jutland.

A study of sediment source at reef sites near the Charleston Ocean dredged material disposal site was carried out using gamma isotope tracers (Noakes, 2004). A total of 10 sediment grab samples were collected in April 2004 from Charleston Harbor, the Cooper river, several small tributaries and near-shore sites along a transect leading towards the disposal area. Analyses of the tributary and harbour sediments had clearly shown that ^{7}Be and ^{137}Cs were associated with terrestrial sediment. The presence of ^{7}Be and ^{137}Cs in the offshore diver collected and sediment trap samples indicated that this sediment was also of terrestrial origin. The study therefore concluded that some terrestrial sediment has been transported to a subset of the hard bottom reef monitoring stations through natural processes.

(x) Marine Research

Tsabaris and Ballas (2004) and Tsabaris et al. (2005) deployed NaI(Tl) based underwater gamma ray spectrometer to measure ^{137}Cs and ^{40}K in open sea at 3 m depth at five sites in Aegean Sea. The volumetric activity of the natural gamma-ray emitter ^{40}K in open sea varied from 12,200 to 13,000 Bq/m^3. The increase in ^{40}K was related to increase in salinity with depth. At one of the sites, the amount of the artificial radioactivity from ^{137}Cs was increased up to seven times higher after strong rainfall, compared to the radiation level as given in literature (3.5–5.5 Bq/m^3). The activity concentration of ^{214}Bi increased up to 991±102 Bq/m^3 after strong rainfall in the North Aegean Sea in winter (humid period) with

east wind direction. On other hand, the maximum activity concentration reached the level of 110±10 Bq/m^3 in summer (dry period) during south winds (Tsabaris, 2008).

(xi) Air Pollution

Air gamma dose rate map of Piemonte, a region in the North-West of Italy, was produced from gamma spectrometry soil data. Soil samples collected in 110 different sites of Piemonte were analyzed with HPGe detectors, which allowed the evaluation of the activity concentrations of natural radionuclides and ^{137}Cs (Losana et al., 2004). Then, using the available mathematical models, the gamma absorbed dose rate in air due to radionuclides was calculated. The contribution of the cosmic radiation to the total absorbed dose rate, which depends on the site altitude was also evaluated and added to the soil contribution. Finally, the map of the whole region was obtained by fitting the dose rate values of the different sites with Kriging algorithms.

Indoor and outdoor in situ high-resolution gamma radiation measurements in urban areas of Cyprus were performed (Soukis and Tsertos, 2007). Specific activities and gamma absorbed dose rates in air due to naturally occurring radionuclides of ^{232}Th, ^{238}U series, and ^{40}K were determined and discussed. Effective dose rate to the Cyprus population due to terrestrial gamma radiation is derived directly from this work. The results obtained outdoors match very well with those derived previously by high-resolution gamma spectrometry of soil samples, which were collected from the main Island bed rock surface. This implies that the construction and building material in urban areas do not affect the external gamma dose rate; thus they are mostly of local origin. Finally, the indoor/outdoor gamma dose ratio was found to be 1.4±0.5.

(xii) Pollution in Precipitation

Landsberger et al. (1983) investigated anthropogenic pollution of urban snow. The trace elements were analyzed by PIXE and instrumental neutron activation analysis (INAA) methods. The snow samples were collected from the island of Montreal and some from Toronto and were filtered to separate soluble and insoluble fractions. A total of twenty-five trace elements (Na, Mg, Al, P, S, CI, K, Ca, Ti, V, Cr, Mn, Fe, Co, Ni, Cu, Zn, As, Se, Br, Rb, Sr, Mo, Cd and Pb) were obtained in the soluble snow portion with detection limits between 0.2 ng/g and 147 ng/g. Twenty-eight elements (Na, Mg, Al, P, S, CI, K, Ca, Sc, Ti, V, Cr, Mn, Fe, Co, Ni, Cu, Zn, As, Se, Br, Rb, Sr, Cd, Sb, La, Sm and Pb) were analyzed with detection limits between 3 µg/g and 720 µg/g in the insoluble particulate matter. On the basis of solubility and enrichment factor, these elements were suggested to be anthropogenic in nature, based on comparison of enrichment factors in both the soluble and insoluble portions of urban snow with those in coal, considered as a typical combustion source of airborne particulates.

In order to investigate environmental pollution due to anthropologic reasons, Hanson et al. (1988) collected monthly precipitation samples in 1984 at four sites in Sweden and analyzed for trace metal using the instruments PIXE and Graphite Furnace AAS (GFAAS). The concentrations of P, S, K, Ca, V, Mn, Fe, Ni, Zn, As, Br and Pb were observed higher than the chemical blank. Good agreement was found between PIXE and GFAAS in determining the elemental concentrations of Cu, Fe, Mn, Pb and Zn. The PIXE technique is also suggested to be promising for Ti, Cr, Cu, Ga, Ge, Se, Rb and Sr.

The concentrations and the concentration ratios of individual short-lived ^{222}Rn decay products (^{214}Pb and ^{214}Bi) in rainwater were measured at Kumatori village in Osaka, Japan, by gamma-ray spectrometry (Takeyasu et al., 2006). It was observed that the concentrations were negatively correlated with the rainfall rate in some rainfall events which was related with the cold front during a single rainfall event. Based on the relationship between the concentrations of ^{214}Pb and ^{214}Bi in the rainwater and the rainfall rate, the increase in the environmental gamma-ray dose rate from ^{214}Pb and ^{214}Bi deposited on the ground was calculated. The calculated increase agreed well with that observed by the in situ measurement on flat ground. In a similar study, Horng and Shiang (2004) estimated radon concentration in raindrops as well as in cloud droplets based on a simplified rainout model from the in situ measurement of gamma ray intensity. From the measured radon progeny concentration in raindrops the additional exposure rate due to rainfall has been evaluated and compared with the HPIC (high pressure ionization chamber) monitoring data.

(xiii) Pollution of Surface Water and Groundwater

Elemental composition of water is of great importance to life. Water provides the essential elements to the living environment. The way it supports the life it can also destroy the life if it gets toxicated. Therefore, water analysis is essential for public and environmental health. Depending upon the purpose of the study and availability of the facility, water is analyzed in different ways in various parts of the world.

To monitor the effluent releases from SRS and plant Vogtle (Georgia Power), Winn (1995) used underwater NaI(Tl) and HPGe detectors to make gamma measure-

ment on the Savannah river. The NaI(Tl) tracked plant Vogtle release for six years which showed dominance ^{58}Co with activity 4 mBq/l. With HPGe detector, ^{137}Cs was found as the dominant gamma emitting source in the SRS cooling pond with activity up to 2.0 mBq/m^2. The contour maps of sediment ^{137}Cs provided guidance for partially draining the ponds for dam repairs.

For the purpose to know the change in radionuclide concentration before and after the start of the nuclear power plant (NPP) operation in, Czech Republic, natural and artificial radionuclides in the area up to distance from 2 to 20 km around NPP was analyzed using HPGe spectrometer (Thinova et al., 2006; Cechak et al., 2000-2004). Processing of measured spectra in the range up to 3 MeV provided mass related activity of naturally radioactive elements ^{40}K, ^{226}Ra, ^{232}Th and contaminant ^{137}Cs produced from nuclear weapon tests and from Chernobyl accident fall out. In situ, NaI(Tl) spectrometer was used for measurement of absorbed dose in water. Environmental samples (Schreber moss, forest humus, pine bark, mushrooms and forest berries) were also analyzed in the laboratory using HPGe gamma spectrometer. For this purpose, air Kerma rate was determined from the measured photon spectra and it was used to get absorb dose rate to water in order to appraise human irradiation.

Jubeli and Parry (1986) measured very low levels of uranium in groundwater from the Palmyrides region, Central Syria, using NAA technique and laser induced fluoremetry. The results obtained by these two techniques were found to be in good agreement.

Holynska et al. (1998) compared total reflection X-ray fluorescence (TXRF) and grazing emission X-ray fluorescence (GEXRF) to determine concentration of Na, Mg, K, Ca, Ni, Cu, Zn and Sr in drinking water and found that TXRF is suitable for heavy elements (Z>19) while GEXRF for low-Z elements.

Mine waste water management is an important problem in the field of environmental protection. Water, penetrating layers of rock mass, dissolves various salts. Kot et al. (2000) analyzed mine water for water quality analysis using XRF-spectrometry with the helium system by semi-quantitative XRF method on the basis of SemIQ program and calibration curves. Portions of 20 cm^3 of mine waters were taken for analysis. Maximum concentration values (in g/dm^3) in the analyzed samples were Na (76), Ca (3), Mg (4), K (1.2), Cl (130), S (0.95) and Al (1.18). The analyzed values by semi-quantitative method were found in good agreement with those obtained by calibration curves method. Cl, Ca and Mg contents measured using volumetric methods also compared well with those obtained by XRF method. The concentrations of Zn, Cr, Cd, Pb and Cu in the tested mine water samples were found lower than the detection limit.

(xiv) Soil Pollution

Losana et al. (2001) compared environmental gamma dose determined using (i) high pressure ionization chamber, (ii) TLD dosimeters, (iii) in situ gamma ray spectrometry and (iv) dose evaluation from the activity concentration of radionuclides in the soil. Soil samples gathered from a field near Turin (North-West Italy) were analyzed with the *p*-type HPGe, and their radionuclide concentrations were used to evaluate the dose at 1 m above the soil surface. At the same location the dose rate was evaluated with the in situ gamma ray spectrometry and with the ionization chamber and the TLD dosimeters. The contribution of cosmic rays was added to the dose rate calculated from the soil samples and the in situ gamma spectrometry. The results obtained with these four techniques agreed well within 20%.

(xv) Hot Springs

Source of heat at the Tarbalu hot water spring in the geothermal region of Eastern Ghats of Orissa was investigated by measuring radioactive concentration in soil and rock samples (Barnawal et al., 2006). Higher and lower energy spectrum of uranium, thorium and potassium were analyzed by NaI(Tl) and HPGe spectrometers respectively. Maximum concentration of ^{238}U, ^{232}Th and ^{40}K were found to be 95 ppm, 1194 ppm and 4 %, respectively in soils and 1434 ppm, 10,590 ppm and 8%, respectively in the granitic rocks. The gamma dose rate in air was approximately 10 times greater than the dose rates obtained outside the high radiation zone. High concentration thorium associated radiogenic heating is suggested to be the dominant source for the subsurface heat and for the observed hot water spring.

(xvi) Dendrochemical Analysis

Dendrochemical analysis provides information concerning the geochemical and atmospheric environment to which the tree has been exposed. Gilfrich et al. (2005) measured elemental concentration in Sassfras and Red Oak using SR-XRF and ED-XRF at concentration up to 1 ppm for nine elements. Major year-to-year variations were observed, implying that cross-ring elemental migration is slow (possibly negligible). Schaumloffel et al. (1999) analyzed tree rings of ponderosa pine along the contaminated water ways. The investigation revealed increased Cd contamination in individual growth ring

according to increase in Cd concentration in water quality of lake water from 1984-1988. Calva-Vazquez et al. (2006) analyzed tree rings of pine and Sacred fur at the surroundings of the Mexico Valley using PIXE. This study provided information about the elemental concentration in trees during the years from 1965 to 2003. The measurements showed some trends for Fe and Zn in the tree-rings elemental composition that may be correlated to recent volcanic activities in the region. The low Mn contents were interpreted as due to soil acidification and the forest decline.

(xvii) Climate Research

All existing ^{10}Be records from Greenland and Antarctica show increasing concentrations during the Maunder Minimum period (MM), 1645–1715, when solar activity was very low and the climate was colder (little ice age). In detail, however, the ^{10}Be records deviate from each other. Heikkila et al. (2008) investigated this using the ECHAM5-HAM general circulation model. ^{10}Be production calculations show that during the MM the mean global ^{10}Be production was higher by 32% than at present due to lower solar activity. The model shows that the zonally averaged ^{10}Be deposition flux deviates by only ~8% from the average increase of 32%, indicating that climatic effects are much smaller than the production change. Due to increased stratospheric production, the ^{10}Be content in the downward fluxes is larger during MM, leading to larger ^{10}Be deposition fluxes in the subtropics, where stratosphere-troposphere exchange (STE) is strongest. In polar regions the effect is small. In Antarctica, the change is larger in the east than in the west. The model calculations point to a stronger STE in the Northern Hemisphere during MM. In the Southern Hemisphere the change is small. These findings indicate that climate changes do influence the ^{10}Be deposition fluxes, but not enough to significantly disturb the production signal. Climate-induced changes remain small, especially in polar regions.

(xviii) Allied Research

In allied applications, Benz et al. (2006) applied X-ray absorption-transmission spectroscopy to monitor water movement in curing process as a function of hydration time. The spatial data was de-convoluted to three dimensional colour coded images to locate water volumes evacuated from the hydrating cement microstructure.

Portable spectrometers are especially important at places where samples are forbidden to transport to laboratory for analysis. Ferreti et al. (2007) used portable XRF attached to Peltier-cooled Si-Drift detector and Laser-Induced Breakdown Spectroscopy (LIBS) for in situ analysis of several bronze pieces belonging to the group of the so-called *Porticello Bronzes*. The find occurred at sea, off the village of Porticello (Reggio Calabria) in 1969 and consists of a number of fragments. The elemental analysis discriminated the artifact in two different statues; the first characterized by the presence of bismuth and relatively high signals of Ag and Pb, possibly connected with the use of argentiferous lead (the 'philosopher'); the second with bismuth below detection limits. The observed elemental differences are related to source difference of the object formation and fabrication context. Thus the work shows the significance of elemental analysis in tracing the origin of an object matrix.

(xix) Bio-Medical Applications

The importance of food as radionuclide source for the *Daphnia magna* was investigated using a planktonic food chain (Adam et al., 2002). Daphnids placed in a tank were fed on algae previously kept for four days in natural water contaminated by ^{110m}Ag, ^{60}Co, ^{137}Cs and ^{54}Mn. After about one week of exposure, daphnids were placed in non-contaminated water on a diet of non-labelled algae, in order to monitor radionuclide release. For the radionuclide transfer via *Cyclotella meneghiana*, the biological periods ranged, for the first compartment, from 7 to 30 min and for the second, from 10 h to 1.8 d. As regards the transfer via the green algae *Scenedesmus obliquus* the biological half-lives were longer.

Radioactive isotopes, especially gamma emitters, are widely used in nuclear medicines. Important among these are: ^{99m}Tc, ^{123}I, ^{201}Tl, ^{133}Xe, ^{81m}Kr, ^{57}Co, ^{137}Cs and ^{111}In. Approximately 85% diagnostic imaging procedures in nuclear medicine use Technetium (^{99m}Tc) isotope. Medical application of some of the nuclear medicines and their radiation properties is given in Table 6 (Lombardi, 2006).

(xx) Lunar and Planetary Environment

The year 2009 marks the 40th year of man's landing on moon. Apollo series continued several moon missions. The in-situ analysis of chemical composition of lunar sample is extensively studied using Gamma ray spectrometer (GRS) and XRF spectrometer in the experiments, *Apollo 15* and *Apollo 16*. The GRS has detected uranium and thorium and also the elements that become gamma rays emitter on bombardment of the lunar surface by galactic cosmic rays. The GRS mapped the abundance of thorium, iron and titanium on 20% of lunar surface. High iron, thorium and titanium abundances are found in all Lunar mare regions (Lawrence et al., 1998).

Table 6: Energy characteristic of some important isotopes used in clinical and diagnostic applications

Isotope	$T_{1/2}$	*Energy (keV) and %*	*Application*
^{99m}TC	6 h	E_γ=140 (89%)	Imaging and functional studies of brain, myocardium, thyroid, lungs, liver, gall-bladder, skeleton, blood and tumors
^{123}I	13.2 h	E_γ=159 and 27	Thyroid diagnosis and in Parkinson's disease
^{201}Tl		E_γ = 135 (2%) and 167 (8%), $K_{x\text{-ray}}$ = 69-83 keV (94%)	Extensively used in myocardial perfusion imaging
^{133}Xe	5.3 d	E_γ = 81 (36%) $E_{x\text{-ray}}$ = 32 (48%)	Lungs treatment
^{81m}Kr	13 s	E_γ=190	Lungs treatment
^{57}Co		E_γ = 123 (89%), 136 (11%)	Lung cancer treatment
^{137}Cs		E_γ = 662 (84%)	3D positron imaging tomography scanning
^{111}In		E_γ = 364 (83%), 638 (9%)	Treatment of tumour

When X-rays from the Sun strike the lunar surface, some elements become X-rays fluorescent. The XRF Spectrometer measured the abundance of the elements magnesium, aluminum and silicon on the lunar surface. In all, about 9% of the Moon's surface was studied by this experiment. The Al/Si ratio is lowest over mare regions and it is a factor of two higher over non-mare regions. High values of Mg/Si ratio tend to occur in mare regions where magnesium in basalts is in the mineral pyroxene. Lower values of the Mg/Si ratio were observed in the plagioclase-rich highland rocks (Heiken et al., 1991). The Chandrayaan-1 lunar mission launched on 22nd October 2008 contains compact X-ray spectrometer (C1XS) designed to measure absolute and relative abundance of major rock-forming elements (principally Mg, Al, Si, Ca and Fe) and other minor elements like Na, P and S on lunar crust with relative elemental abundance better than 10%. This will provide an insight into lunar evolution (Grande et al., 2009). The C1XS contains Swept Charge Device detectors that has high detection efficiency in the range 0.8-7 keV. It has spatial resolution £ 25FWHM km, working energy range is 0.8–20 keV and the energy resolution 200 eV FWHM at 8 keV (2%).

GRS of Mars Odyssey found distinctive signatures of hydrogen on some areas of Martian surface which was later confirmed by mission Phoenix (launched in August 2007) that the source of hydrogen is ice frozen below the surface (Smith et al., 2009).

(xxi) Celestial Matter

Celestial gamma-ray line studies are capable of identifying electron-positron annihilation emission, can detect radioactivity from supernova and radioactive tracer isotopes generated in cosmic nucleosynthesis events, active galactic nuclei pulsars, dark matter and can provide insights into the interior processes of massive-star gravitational collapses (Leising and Diehl, 2008). Gamma-ray Large Area Telescope (GLAST) is intended to observe some of these phenomena. It was launched aboard on Delta II rocket on 11 June 2008. It contained two detectors: (i) Large Area Telescope: to detect photons with energy from 30 MeV to 300 GeV with a field of view of about 20% of the sky and (ii) Gamma-ray Burst Monitor that contained 14 scintillation detectors [twelve sodium iodide (NaI(Tl) crystals for the 8 keV to 1 MeV range and two bismuth germanate (BGO) crystals with sensitivity from 150 keV to 30 MeV] to detect gamma-ray bursts across the whole of the sky not occulted by the Earth. The mission is a joint venture of NASA, US Dept. of Energy, and government agencies in France, Germany, Italy, Japan and Sweden (Ref.: http).

Conclusion

In the present paper, we have described in detail instrumental methods for determination of inorganic elements and radioisotope in the environment. After providing the details of XRF, PIXE, NAA, and gamma ray detectors (NaI(Tl), Si(Li), Ge(Li), HPGe and SDD) we tried to popularize these techniques through illustrating many. These include studies on: contamination of air, water and soil; sediment transport, erosion and deposition; leakage in reservoirs, well logging, water equivalent of snow, coastal currents and marine research; atmospheric and climatic research; archeology; bio-medical applications and environment outside earth including deep space. These illustrations

would certainly help the scientific community to further investigate more diverse and critical cases. This in turn would bring more refinement in the instrumental technology through its automation, lowering of detection limit and portability for in situ measurements.

References

Adam, C., Garnier-Laplace, J. and J.P. Baudin (2001). Bioaccumulation of ^{110m}Ag, ^{60}Co, ^{137}Cs and ^{54}Mn by the Freshwater Crustacean *Daphnia magna* from Dietary sources *(Scenedesmus obliquus* and *Cyclotella meneghiana*). *Water, Air and Soil Pollution*, **136:** 125-146.

Adams, F., Janssens, K. and A. Snigirev (1998). Microscopic X-ray fluorescence analysis and related methods with laboratory and synchrotron radiation sources. *French Journal of Analytical Atomic Spectrometry*, **13:** 319-331.

Akram M., Qureshi, R.M., Ahmed, N. and T.J. Solaija (2006). Gamma emitting radionuclides in the shallow marine sediments off the Sindh Coast, Arabian Sea. *Radiat. Prot. Dosim*., **118(4):** 440-447.

Andreu Ibarra, B., Galvez Cruz, L., Ruiz Pena, O. and R. Del Arenal (1978). Estudio isotopic de las fugas de la presa Las Lajas, Chihuahua, Mexico. *Proc. Symp. Neuherberg*, 1978, IAEA, Vienna.

Arnold, D.M. (1995). Oxygen activation method for quantitative water flow measurements within and behind well bore casing. US Patent 5461909, October 31.

Avdyushin, S.I. et al. (1979). Experience of snow water equivalent measurement in mountainous by galactic cosmic radiation absorption. *Meteorl. Hydrol*., **12:** 9.

Bacchi, O.O.S., Reichardt, K., Oloveira, J.C.M. and D.R. Nielsen (1998). Gamma-ray beam attenuation as an auxiliary technique for the evaluation of the soil water retention curve. *Sci. Agric*., **55(3):** Piracicaba, Scientia Agricola.

Baranwal, V.C., Sharma, S.P., Sengupta, D., Sandilya, M.K., Bhaumik, B.K., Guin, R. and S.K. Saha (2006). A new high background radiation area in the Geothermal region of Eastern Ghats Mobile Belt (EGMB) of Orissa, India. *Radiation Measurements*, **41:** 602-610.

Barataud, F., Christian, M. and D. Stemelen (1999). Measurement of Soil Water Diffusivity of an Undisturbed Forest Soil Using Dual-Energy Gamma Radiation Technique. *Soil Science*, **164:** 493-502.

Benz, D.P., Halleck, P.M., Grader, A.S. and J.W. Roberts (2006). Four dimensional X-ray tomography study of water movement during internal curing. *In:* Proceedings of the International RILEM Conference. (Eds.) O.M. Jensen, P. Lura and K. Kovler, RILEM Publ. S.A.R.L., Baneux, France.

Bland, W.L., Helmke, P.A. and J.M. Baker (1997). High-resolution snow-water equivalent measurement by gamma-ray spectroscopy. *Agricultural and Forest Meteorology*, **83:** 27-36.

Burnett, W.C. and H. Dulaiova (2003). Estimating the dynamics of groundwater input into the coastal zone via continuous radon-222 measurements. *Journal of Environmental Radioactivity*, **69:** 21-35.

Calva-Vázquez, G., Razo-Angel, G., Rodríguez-Fernández, L. and J.L. Ruvalcaba-Sil (2006). Study of $Z > 18$ elements concentration in tree rings from surrounding forests of the Mexico Valley using external beam PIXE Ion Beam Analysis. *Nuclear Instruments and Methods in Physics Research Section B: Beam Interactions with Materials and Atoms*, **249:** 588-591.

Cechak, T., Kluson, J., Thinnova, L. and T. Trojek. (2000-2004). Bio-monitoring of radionuclide atmospheric deposits in the neighborhood of NPP. *Temlin Research Report*, CTU, Prague-CR, 55 pages.

Chen, Y., Kashy, E., Bazin, D., Benenson, W., Morrissey, D.J., Orr, N.A., Sherrill, B.M., Winger, J.A., Young, B. and J. Yurkon (1993). Half life of ^{32}Si. *Physical Review*, **C. 47:** 1462-1465.

Christensen, G.C., Bergen, T.D.S., Berge, D. and T. Baekken (1988). A comparison of seawater and freshwater in the study of sediment-water exchange of radionuclides. *Radiation Protection and Dosimetry*, **75**: 107-109.

Church, T.M., Bernat, M. and P. Sharma (1986). Distribution of natural uranium, thorium, lead and polonium radionuclides in tidal phases of a Delaware Salt Marsh. *Estuaries*, **9(1):** 2-8.

Crickmore, M.J., Tazioli, G.S., Appleby, P.G. and F. Oldfield (1990). The use of nuclear techniques in sediment transport and cementation problems. Technical Documents in Hydrology, IHP-III Project, Paris, UNESCO, 170 p.

Dahlgaard, H. (1995). Radioactive tracers as a tool in coastal oceanography: An overview of the MAST-52 Project. *Journal of Marine Systems*, **6:** 5-6, 381-389.

Demir, D., Ün, A., Özgül, M. and Y. Sahin (2008). Determination of photon attenuation coefficient, porosity and field capacity of soil by gamma-ray transmission for 60, 356 and 662 keV gamma rays. *Applied Radiation and Isotopes*, **66:** 1834-1837.

Danilin, A.I. and B.T. Dubinchuk (1983). Water equivalent of snow cover. Guidebook on nuclear techniques in hydrology. Technical Report Series No. 91, IAEA, Vienna, 35-63.

Du, J., Zhang, J., Zhang, J. and Wu Y. Yunfeng (2008). Deposition patterns of atmospheric ^{7}Be and ^{210}Pb in coast of East China Sea, Shanghai, China. *Atmospheric Environment*, **42:** 5101-5109.

Drost, W. and H. Moser (1983). Leakage from lakes and reservoirs. Guidebook on nuclear techniques in hydrology. Technical Report Series No. 91, IAEA, Vienna, 177-186.

Fanger, H.U. and Pepelnik, R. (1975). Exploration of uranium ore deposits utilizing spectroscopy of neutron induced gamma radiation. Tire A: part de la Review Industries Atomiques & Spatial, No. 4 39, *Rule Pellonuer*, 122, Genevel Cheni-Burg/Suisse.

Fifield, L.K. and U. Morgenstern (2009). Silicon-32 as a tool for dating the recent past. *Quaternary Geochronology* (doi:10.1016/j.quageo.2008.12.006 on line).

Ferretti, M., Cristoforetti, G., Legnaioli, S., Palleschi, V., Salvetti, A., Tognoni, E., Console, E. and P. Palaia (2007). In situ study of the *Porticello Bronzes* by portable X-ray fluorescence and laser-induced breakdown spectroscopy. *Spectrochimica Acta Part B: Atomic Spectroscopy*, **63:** 1512-1518.

Fridman, Sh. D. (1968). The cosmic radiation technique of measuring the snow cover water equivalent in mountains. *Meteorol. Hydrogeol*., **6:** 84.

Fridman, Sh. D. (1979). The use of cosmic radiation absorption for measuring the water equivalent of snow. Nuclear and isotope techniques in the study of natural waters. An UUSR, Moskow, 67.

Folsom, T.R. and C. Sreekuman (1970). Reference methods for marine radioactivity studies. IAEA Bulletin.

Gilfrich, J.V., Gilfrich, N.L., Skelton, E.F., Kirkland, J.P., Qadri, S.B. and D.J. Nagel (2005). X-ray fluorescence analysis of tree rings. *X-ray Spectrometry*, **20:** 203-208.

Goldstein, J., Newbury, D.E., Joy, D.C., Lyman, C.E., Echlin, P., Lifshin, E., Sawyer, L.C. and J.R. Michael (2007). Scanning Electron Microscopy and X-ray Microanalysis, Springer Publ. 3rd Ed. Corr 4th Printing, 586 p.

Grande, M. and 29 co-authors (2009). The C1XS X-ray Spectrometer on Chandrayaan-1. *Planetary and Space Science,* **57:** 717-724.

Gudiksen, P.H., Harvey, T.F. and R. Lange (1989). Chernobyl source term, atmospheric dispersion, and dose estimation. *Health Physics*, **57:** 5697-5706.

Guiles, J.R. and K.J. Dooley (1998). High resolution gamma spectroscopy well logging system. *Journal of Radioanalytical and Nuclear Chemistry*, **233:** 125-130.

http://www.nasa.gov/mission_pages/GLAST/news glast_gbm.html

Hanson, H.C., Ekholm, A.K.P. and H.B. Rose (1988). Rainwater Analysis: A comparison between Proton Induced X-ray Emission and Graphite Furnace Atomic Absorption Spectroscopy. *Environmental Science and Technology*, **22:** 527-531.

Harman, J., Kershaw, P.J., Bailly du Bois, P. and P. Guegueniat (1995). The distribution of artificial radionuclides in the English Channel, Southern North Sea, Skagerrak and Kattegat. *Journal of Marine Systems*, **5-6:** 427-456.

Heikkila, U., Beer, J. and J. Feichter (2008). Modelling cosmogenic radionuclides ^{10}Be and ^{7}Be during the Mounder minimum using the ECHAM5-HAM general circulation model. *Atmospheric Chemistry and Physics*, **8:** 2797-2809.

Heiken, G.H., Vaniman, D.T. and B.M. French (1991). Lunar Sourcebook: A User's Guide to the Moon. Cambridge University Press.

Holynska, B., Olko, M., Ostachowicz, B., Ostachowicz, J., Wegrzynek, D., Claes, M., Grieken, R.V., de Bokx, P., Kump, P. and M. Neceme (1998). Performance of total reflection and grazing emission X-ray fluorescence spectrometry for the determination of trace metals in drinking water in relation to other analytical techniques. *Fresenius Journal of Analytical Chemistry*, **362:** 294-298.

Horng, M.C. and S.H. Jiang (2004). In situ measurements of gamma ray intensity from radon progeny in rainwater. *Radiation Measurements*, **38(1):** 23-30.

Jha, S.K., Chavan, S.B., Pandit, G.G. and S. Sadasivan (2003). Geochronology of Pb and Hg pollution in a coastal marine environment using global fall out ^{137}Cs. *Journal of Environmental Radioactivity*, **69(1, 2):** 145-157.

Jubeli, Y.K. and S.J. Parry (1986). A new application of neutron activation analysis with 239U to determine uranium in groundwater. *Jrl. of Radioanalytical Nucl.Chem.*, **102:** 337-346.

Kogan, R.M., Nazarov, M.D. and I.M. Fridman (1976). Fundamentals of gamma spectrometry of natural environments. Atomizdat, Moskow, 336 pages.

Kot, B., Baranowski, R. and A. Rybak (2000). Analysis of mine waters using X-ray fluorescence spectrometry, *Polish Journal of Environmental Studies*, **9:** 429-431.

Kumar, B. et al. (2005). Evaluation of recent trends of sedimentation in Indian lakes using ^{210}Pb and ^{137}Cs dating technique. Urban Lakes in India: Conservation, Management and Rejuvenation, Part I: 135-145, National Institute of Hydrology, Roorkee, India.

Knoth, J., Marten, R., Schneider, H. and H. Schweike (1976). On line determination of heavy materials in marine deposits by X-ray spectrometry, Gesellschaft fur Kernenergie ver wertung in Schiffbau und Schiffahrt mbh Io 76-105/01.

Lal, D., Arnold, J.R. and B.L.K. Somayajulu (1968). A method for the extraction of trace elements from sea water. *Geochimica, Cosmochimica, Acta*., **28:** 1111-1116.

Lal, D., Goldberg, E.D. and M. Koide (1960). Cosmic ray produced ^{32}Si in nature. *Science*, **131:** 332-337.

Lal, D., Nijampurkar, V.N., Somayajulu, B.L.K., Koide, M. and E.D. Goldberg (1976). Silicon-32 specific activities in coastal waters of the world oceans. *Limnology and Oceanography*, **21(2):** 285-293.

Lal, D. (1998). Cosmic ray produced isotopes in terrestrial systems. *Journal of Earth System Science*, **107:** 241-249.

Landsberger, S., Jervis, R.E., Kajrys, G. and S. Monaro (1983). Characterization of trace elemental pollution in urban snow using Proton Induced X-ray emission and Instrumental Neutron Analysis. *International Journal of Environmental Analytical Chemistry*, **16:** 95-113.

Lawrence, D.J., Feldman, W.C., Barraclough, B.L., Binder, A.B., Elphic, R.C., Maurice, S. and D.R. Thomsen (1998). Global Elemental Maps of the Moon: The Lunar Prospector Gamma-Ray Spectrometer. *Science*, **281:** 1484-1489.

Leising, M. and Diehl (2008). Gamma-Ray Line Studies of Nuclei in the Cosmos *10th Symposium on Nuclei in the Cosmos*, July 27-August 1 2008, Mackinac Island, Michigan, USA.

Lombardi, M.M. (2006). Radiation safety in nuclear medicine. CRC Press, Boca Raton, Fl., USA, 2nd Edition, 231 p.

Losana, M.C., Mangnoni, M. and F. Righino (2001). Comparison of different methods for the assessment of the environmental gamma dose. *Radiation Protection Dosimetry*, **97:** 333-336.

Losana, M.C., Magnoni, M., Bertino, S., Procopio, S., Facchinelli, A. and E. Sacchi **(**2004). Gamma dose rate calculation and mapping of piemonte (North-West Italy) from gamma spectrometry soil data. *Radiation Protection Dosimetry*, **111(4):** 419-422.

Makowski, J. (1967). Radiometric method of seepage control in dams and their environs. Isotope in hydrology. Proc. Symp. Vienna, 1966, IAEA, Vienna, 601.

Makowski, J. (1970). Radiometric method for investigating the permeability of reservoir beds. Isotope Hydrology, Proc. Symp. Vienna, 1970, IAEA, Vienna, 727.

Mason, Brion (1966), Principles of Geochemistry. John Willey, New York.

McCulloch, J. (1983). Soil density. Guide book on nuclear techniques in hydrology. Technical Report Series No. 91, IAEA, Vienna.

Mettler, F.A. (2008). Public/worker/patient health protection and CVD, radiation risks. Beebe Symposium Washington DC. December 3, 2008.

Molinari, J., Guizerx, J. and R. Chmbard (1970). Nouvelle method de localization de fuites sur des reservoirs ou Cannaux au moyen d'emulsion d'emulsion de bitume marque. Isotope Hydrology, Proc. Symp. Vienna, 1970, IAEA, Vienna, 743.

Moore, W.S. and D.F. Reed (1973). Extraction of radium from natural waters using manganese-impregnated acrylic fibers. *Journal of Geophysical Research*, **78:** 8880-8885.

Nielson, K.K., Thomas, C.W., Wogman, N.A. and R.L. Brodzinski (1976). Development of a plutonium-americium monitor for in-situ soil surface and pond bottom assay. *Nucl. Instruments Methods*, **138:** 227-234.

Niedermayr, T., Vetter, K., Mihailescu, L., Schmid, G.J., Beckedahl, D., Blair, J. and J. Kammeraad (2005). Gamma-ray imaging with a coaxial HPGe detector. *Nuclear Instruments and Methods in Physics Research*, **A553:** 501-511.

Noakes, S. (2004). Utilizing gamma isotope tracers to determine sediment source at reefs site near the Charleston Ocean dredged material disposal site. Report submitted to South Carolina Department of Natural Resources, Marine Resources Division, 217 Fort Johnson Road, Charleston, SC 29412-2559.

Osterberg, C., Cutshall, N. and J. Cronin (1965). Chromium-51 as a radioactive tracer of Columbia river water at sea. *Science*, **150:** 3703, 1585-1587.

Povinec, P.P., Bokuniewicz, H., Burnett, W.C., Cable, J., Charette, M., Comanducc, J.-F., Kontar, E.A., Moore, W.S., Oberdorfer, J.A., de Oliveira, J., Peterson, R., Stieglitz, T. and M. Taniguchi (2008). Isotope tracing of submarine groundwater discharge offshore Ubatuba, Brazil: Results of the IAEA-UNESCO SGD project. *Journal of Environmental Radioactivity*, **99:** 1596-1610.

Rai, S.P., Vijay Kumar and Bhishm Kumar (2007). Sedimentation rate and pattern of a Himalayan foothill lake using ^{137}Cs and ^{210}Pb. *Hydrological Science Journal*, **52(1):** 181-191.

Rieck, H.G., Kosorrok, J.R., Perkins, R.W. and N.A. Wogman (1975). In situ X-ray fluorescence design. BNWL-B-395, Battelle, Pacific Northwest Laboratories, Richland, Washington, USA.

Saxena, D.P., Jose, P., Van Grieken, R. and V. Subramanian (2002). Sedimentation rate of the flood plain sediments of the Yamuna river basin (tributary of the river Ganges, India) by using ^{210}Pb and ^{137}Cs techniques. *Journal of Radioanalytical and Nuclear Chemistry*, **251:** 399-408.

Schoenfelder, V. (1973). *Nuclear Instruments and Methods*, **107:** 385-390.

Schaumloffel, J.C., Filby, R.H. and B.C. Moore (1996). Instrumental neutron activation analysis of tree rings for dendrochemical studies. *Journal of Radioanalytical and Nuclear Chemistry*, **207:** 425-435.

Silker, W.B. (1975). Collection and analysis of radionuclides in seawater. *In:* Advances in Chemistry, Series No. 147. Analytical Methods in Oceanography, American Chemical Society, 298 pages.

Silker, W.B., Perkins, R.W. and H.G. Rieck (1971). A sampler for concentrating radionuclides from natural waters. *Ocean Engineering*, **2:** 49.

Smith et al. (+24 co-authors) (2009). H_2O at the Phoenix Landing Site. *Science*, **325:** 58-61.

Strüder, L., Lechner, P. and P. Leutenegger (1998). Silicon drift detector–The key to new experiments. *Naturewissenchaften*, **85:** 539-543.

Svoukis, E. and H. Tsertos (2007). Indoor and outdoor in situ high-resolution gamma radiation measurements in urban areas of Cyprus. *Radiation Protection Dosimetry*, **123:** 384-390.

Thinnova, L., Cechak, T., Kluson, J. and T. Trojek (2006). Use of gamma spectrometry method for environmental monitoring in the area of NPP. *Journal of Physics, Conf. Series*, **41:** 569-572.

Tazioli, G.S. (1981). Nuclear techniques for measuring sediment transport in natural streams – Examples from instrumented basins. *Erosion and Sediment Transport Measurement* (Proceedings of the Florence Symposium, IAHS Publ. no. 133.

Todd, R.W., Nightingale, J.M. and D.B. Everett (1974). A proposed γ-camera. *Nature*, **251:** 132.

Takeyasu, M., Iida, T., Tsujimoto, T., Yamasaki, K. and Y. Ogawa (2006). Concentrations and their ratio of ^{222}Rn decay products in rainwater measured by gamma-ray spectrometry using a low-background Ge detector. *Journal of Environmental Radioactivity*, **88:** 74-89.

Tsabaris, C. and D. Ballas (2004). On line gamma ray spectrometry in open sea. *Applied Radiation and Isotopes*, **62:** 83-89.

Tsabaris, C., Thanos, I. and Th. Dakladas (2005). The development and application of an underwater γ-spectrometer in the marine environment. *Radioprotection*, Suppl. 1, **40:** S677-S683.

Tsabaris, C. (2008). Monitoring natural and artificial radioactivity enhancement in the Aegean Sea using floating measuring systems. *Applied Radiation and Isotopes*, **66:** 1599-1603.

UNSCEAR (2000). Sources and effects of ionizing radiations. Report to General Assembly, with Scientific Annexes, United Nations, New York.

Walling, D.E., Woodward, J.C. and A.P. Nicholas (1993). A multi-parameter approach to fingerprinting suspended-sediment sources. *In:* Tracers in Hydrology (Proceedings of the Yokohama Symposium, July 1993) *IAHS Publ. no*. 215, 1993.

Walling, D.E., He, Q. and W. Blake (1999). Use of ^{7}Be and ^{137}Cs measurement to document short and medium term rates of water induced soil erosion on agricultural lands. *Water Resources Research*, **35:** 3865-3874.

Winn, W.G. (1995). Environmental measurements at the Savannah River site with underwater gamma detectors. *Journal of Radioanalytical and Nuclear Chemistry*, **194:** 345-350.

Wegrzynek, W., Markowicz, A., Bamford, S., Chenea-cano, E. and M. Bogovac (2005). Micro-beam X-ray fluorescence and absorption imaging technique at the IAEA Laboratories. *Nucl. Instr. and Methods in Phys. Res*. Sec. B: Beam Interactions with materials and atoms, **231(1-4):** 176-182.

Wogman, N.A., Rieck, H.G., Kosorok, J.R. and R.W. Perkins (1973). In situ activation analysis of marine sediments with ^{252}Cf. *Journal of Radioanalytical Chem*., **15:** 591-600.

Yibo, W., Genxu, W., Hongchang, Hu and C. Huiyan (2008). Erosion rates evaluated by the ^{137}Cs technique in the high altitude area of the Qinghai Tibet plateau of China. *Environmental Geology*, **53:** 1743-1749.

Yujin, Qi, Tsui, B.M.W., Yoder, B. and E.C. Frey (2002). Characteristics of compact detectors based on pixellated NaI(Tl) crystal arrays. *Nuclear Science Symposium Conference Record, IEEE*, **3(10-16):** 1538-1542.

Asian Journal of Water, Environment and Pollution

Volume 7 Number 1 **January – March, 2010**

Contents